The Astrophysical Journal, 696:920–923, 2009 May 1 doi:10.1088/0004-637X/696/1/920

DETECTING THE MILKY WAY'S DARK DISK

Tobias Bruch[1], Justin Read[2], Laura Baudis[1], and George Lake[2]
[1] Physics Institute, University of Zürich, Winterthurerstrasse 190, CH-8057 Zürich, Switzerland; tbruch@physik.uzh.ch, justin@physik.uzh.ch, lbaudis@physik.uzh.ch, lake@physik.uzh.ch
[2] Institute for Theoretical Physics, University of Zürich, Winterthurerstrasse 190, CH-8057 Zürich, Switzerland
Received 2008 October 7; accepted 2009 February 2; published 2009 April 20

ABSTRACT

In the standard model of disk galaxy formation, a dark matter disk forms as massive satellites are preferentially dragged into the disk plane and dissolve. Here, we show the importance of the dark disk for direct dark matter detection. The low velocity of the dark disk with respect to the Earth enhances detection rates at low recoil energy. For weakly interacting massive particle (WIMP) masses $M_{\rm WIMP} \gtrsim 50$ GeV/c^2, the detection rate increases by up to a factor of 3 in the 5–20 keV recoil energy range. Comparing this with rates at higher energy is sensitive to $M_{\rm WIMP}$, providing stronger mass constraints particularly for $M_{\rm WIMP} \gtrsim 100$ GeV/c^2. The annual modulation signal is significantly boosted and the modulation phase is shifted by ∼3 weeks relative to the dark halo. The variation of the observed phase with recoil energy determines $M_{\rm WIMP}$, once the dark disk properties are fixed by future astronomical surveys. The constraints on the WIMP interaction cross section from current experiments improve by factors of 1.4–3.5 when a typical contribution from the dark disk is included.

Key words: dark matter – Galaxy: formation

Online-only material: color figure

1. THE MILKY WAY'S DARK DISK

A mysterious dark matter dominates the matter content of the universe. Although there are no dark matter candidates in the standard model, they are plentiful in extended models. Among these, weakly interacting massive particles (WIMPs; Lee & Weinberg 1977; Gunn et al. 1978; Ellis et al. 1984), which may arise in supersymmetric extensions of the standard model (SUSY; Jungman et al. 1996) or in theories that include universal extra dimensions (Cheng et al. 2002; Hooper & Profumo 2007), stand out as well motivated and detectable.

WIMPs may be detected directly by scattering in a laboratory detector (Goodman & Witten 1985) or indirectly by their annihilation products from their highest density regions (Silk & Srednicki 1984; Lake 1990). In the case of direct detection, we must know the dark matter's phase space structure to predict rates. In early calculations, the standard halo model (SHM) of the dark matter assumed no rotation and the density distribution was taken to be a spherical isothermal sphere with a core radius of several kpc. More recent modeling includes the cuspier central profiles from Λ cold dark matter (ΛCDM) simulations (Navarro et al. 1997; Moore et al. 1998), producing changes of $O(10\%)$ with respect to the SHM (Kamionkowski & Kinkhabwala 1998). Larger boosts have been claimed if dark matter is highly clumped (Green 2002), but it is more likely that we live outside a clump, leading to a modest reduction in the local density (Kamionkowski & Koushiappas 2008).

Simulations containing only dark matter particles have extremely high resolution, but they may not be addressing the "next to leading order" of the model because they do not include the effect of the baryons. Read et al. (2008) recently demonstrated that massive satellites are preferentially dragged into the baryonic disk plane by dynamical friction where they dissolve leaving a thick dark matter disk (Read et al. 2008; Lake 1989). The precise properties of the dark disk depend on the stochastic merger history and cosmology. However, given the expected merger history for a typical Milky Way in ΛCDM, they found a dark disk with density in the range $\rho_{\rm d}/\rho_{\rm h} \sim 0.2$–1 at the solar neighborhood (where $\rho_{\rm h}$ is the density of the SHM). The lower bound $\rho_{\rm d}/\rho_{\rm h} = 0.2$ is particularly conservative since it is produced by just one merger of Large Magellanic Cloud mass within 20° of the disk plane. In ΛCDM, we expect *two* such low inclination mergers per Milky Way (and seven in total at all inclinations).

We may obtain an upper bound on $\rho_{\rm d}/\rho_{\rm h}$ from the kinematics of stars at the solar neighborhood (Oort 1932; Bahcall 1984). The latest measurements from *Hipparcos* give a conservative upper bound of $\rho_{\rm d}/\rho_{\rm h} < 3$, including systematic errors (Holmberg & Flynn 2000; Statler 1989), with $\rho_{\rm d}/\rho_{\rm h}$ being <2 likely. If more than half of the thick disk owes to accretion, the likely dark disk density would be near the upper limit. As such we consider $\rho_{\rm d}/\rho_{\rm h} = [0.5,\ 1,\ 2]$ in this paper. The disk density $\rho_{\rm d}$ is an excess over $\rho_{\rm h}$, locally increasing the dark matter density.

The kinematic properties of the dark disk can be estimated from the accreted stellar thick disk that forms concurrently. Stellar thick disks are found in the Milky Way and in all well-observed spiral galaxies (Burstein 1979; Gilmore & Reid 1983; Yoachim & Dalcanton 2006), while at least one *counterrotating* thick disk is strong evidence for an accretion origin (Yoachim & Dalcanton 2005). However, thick disks can also form through heating of an underlying thin disk (Kazantzidis et al. 2008), or even directly from extended gas (Brook et al. 2004); indeed it is difficult in ΛCDM to obtain a thick disk massive enough from accretion alone (Read et al. 2008). In this paper, we assume—based on the numerical models of Read et al. (2008)—that the dark disk's kinematics match the Milky Way's stellar thick disk. At the solar neighborhood, this gives a rotation lag $v_{\rm lag}$ of 40–50 km s^{-1} with respect to the local circular velocity, and dispersions of $(\sigma_R,\ \sigma_\phi,\ \sigma_z) = (63,\ 39,\ 39)$ km s^{-1} (Read et al. 2008). Since the dispersions are nearly isotropic and somewhat uncertain, we model the dark disk with a simple one-dimensional Maxwellian distribution, with a dispersion and lag, $\sigma = v_{\rm lag} = 50$ km s^{-1}, to show its general effect on direct detection. Improving on this assumption will involve

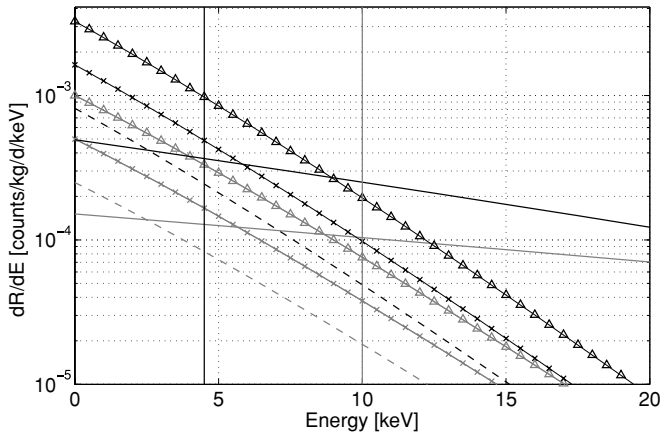

Figure 1. Differential recoil rates for Ge (red/gray) and Xe (blue/black) targets, for $M_{\rm WIMP} = 100$ GeV/c^2 and $\sigma_{\rm (WIMP,N)} = 10^{-8}$ pb in the SHM (solid line) and the dark disk. Three different values of $\rho_{\rm d}/\rho_{\rm h}$ (0.5 dashed, 1 ×, and 2 △) are shown. The vertical lines mark current experiment thresholds: XENON10 (blue/black) using a Xe and CDMS-II (red/gray) using a Ge target.

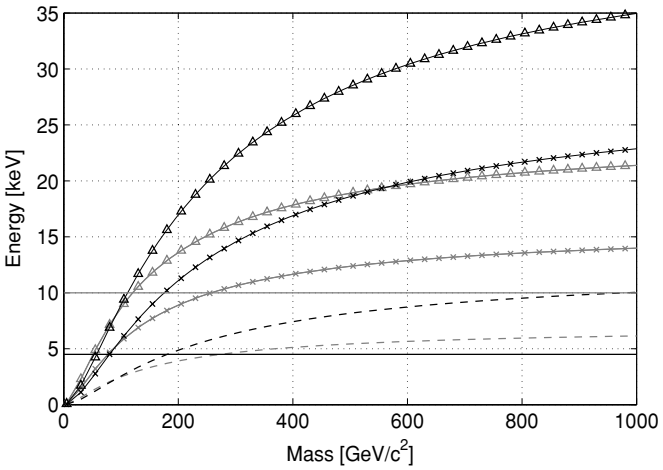

Figure 2. Recoil energy below which the signal is dominated by the dark disk (compared with the SHM) as a function of $M_{\rm WIMP}$ for Ge (red/gray) and Xe (blue/black) targets. Three different values of $\rho_{\rm d}/\rho_{\rm h}$ (0.5 dashed, 1 ×, and 2 △) are shown. The horizontal lines mark current experiment thresholds: XENON10 (blue/black) using a Xe and CDMS-II (red/gray) using a Ge target.

untangling heated versus accreted components in the Milky Way stellar thick disk. This should become possible with future astronomical surveys like the Radial Velocity Experiment (RAVE) (Steinmetz et al. 2006) and *Global Astrometric Interferometer for Astrophysics* (Perryman et al. 2001) that will provide full six-dimensional phase space and chemical information for hundreds of thousands of individual stars.

We emphasize that the dark disk must form in any hierarchical model of structure formation; it is not special to our ΛCDM simulations (Read et al. 2008). However, ΛCDM is specific enough to predict the dark disk density with uncertainties owing only to the stochastic nature of the merging and accretion history. The dark disk is very different from dark matter streams (Freese et al. 2004; Savage et al. 2006) that have a low filling factor (we are not likely to live in a stream), and are stochastic *microstructure*. By contrast, the dark disk is the expected equilibrium end state of dissolving satellites and the Earth *must* be embedded in one (if hierarchical formation is correct). Like the near-spherical dark matter halo, the dark disk is *macrostructure*.

2. DIRECT DETECTION AND THE DARK DISK

Direct detection experiments measure nuclear recoil rates above the detector's energy threshold (Baudis 2006); here we consider Ge and Xe. The detected elastic WIMP–nucleon recoils will range from a few to tens of keV. The expected recoil rate per unit mass, unit nuclear recoil energy, and unit time are (Lewin & Smith 1996)

$$\frac{dR}{dE} = \frac{\rho\sigma_{\rm (WIMP,N)}|F(E)|^2}{2M_{\rm WIMP}\mu^2}\int_{v>\sqrt{mE/2\mu^2}}^{v_{\rm max}}\frac{f(\mathbf{v},t)}{v}d^3v, \qquad (1)$$

where ρ is the local dark matter density ($\rho_{\rm h} = 0.3$ GeV cm^{-3} in the SHM), $\sigma_{\rm (WIMP,N)}$ is the WIMP–nucleus scattering cross section, $F(E)$ is the nuclear form factor, $M_{\rm WIMP}$ and m are the masses of the dark matter particle and of the target nucleus, respectively, μ is the reduced mass of the WIMP–nucleus system, $v = |\mathbf{v}|$ and $v_{\rm max}$ is the maximal velocity in the Earth frame for particles moving at the galactic escape velocity $v_{\rm esc} = 544$ km s^{-1} (Smith et al. 2007). We only consider the spin-independent (SI) scalar WIMP–nucleus coupling in this paper, since it dominates the interaction (depending however on the dark matter particle) for target media with nucleon number $A \gtrsim 30$ (Jungman et al. 1996). We model the velocity distributions of particles in the dark disk and the SHM with a simple one-dimensional Maxwellian:

$$f(\mathbf{v},t) \propto \exp\left(\frac{-(\mathbf{v}+\mathbf{v}_\oplus(t))^2}{2\sigma^2}\right), \qquad (2)$$

where $\mathbf{v}$ is the laboratory velocity of the dark matter particle and the instantaneous streaming velocity $\mathbf{v}_\oplus = \mathbf{v}_{\rm circ} + \mathbf{v}_\odot + \mathbf{v}_{\rm orb}(t)$. This streaming velocity is the sum of local circular velocity $\mathbf{v}_{\rm circ} = (0, 220, 0)$ km s^{-1}, the peculiar motion of the Sun $\mathbf{v}_\odot = (10.0, 5.25, 7.17)$ km s^{-1} (Dehnen & Binney 1999) with respect to $\mathbf{v}_{\rm circ}$, and the orbital velocity of the Earth around the Sun $\mathbf{v}_{\rm orb}(t)$. In the SHM, the halo has no rotation and the dispersion $\sigma = |\mathbf{v}_{\rm circ}|/\sqrt{2}$. For the dark disk, the velocity lag $\mathbf{v}_{\rm lag} = (0, 50, 0)$ km s^{-1} replaces $\mathbf{v}_{\rm circ}$ and a dispersion of 50 km s^{-1} is adopted.

The lower relative velocities of the dark disk significantly increase the differential rate at low energies compared with the SHM rate (Figure 1). Detection of the dark disk crucially depends on the detector's low energy threshold. The differential rate for a specific WIMP target depends on $M_{\rm WIMP}$. In Figure 2, we show the energy below which the dark disk dominates the rate as a function of $M_{\rm WIMP}$, for three values of $\rho_{\rm d}/\rho_{\rm h}$. The total rate in a detector is the sum of the two contributions from the SHM and the dark disk, which dominate at high and low energies, respectively. For $M_{\rm WIMP} \gtrsim 50$ GeV/c^2, the dark disk contribution lies above current detector thresholds, giving a much greater change in the detection rate with recoil energy compared with the SHM alone.

The total rate in a detector using a Ge target is shown in Figure 3 varying $\rho_{\rm d}/\rho_{\rm h}$ and $M_{\rm WIMP}$. If the detectors threshold is sufficiently low even an extremely conservative dark disk with $\rho_{\rm d}/\rho_{\rm h} = 0.1$ can be detected. Current germanium detectors achieve thresholds below 1 keV (Lin et al. 2009; Aalseth et al. 2008). The details of the differential rate with energy, as shown in Figure 3, betray both the contribution of the dark disk relative to the SHM and $M_{\rm WIMP}$. This introduces a mass-dependent characteristic shape of the differential rate which will improve the constrains on $M_{\rm WIMP}$ upon detection.

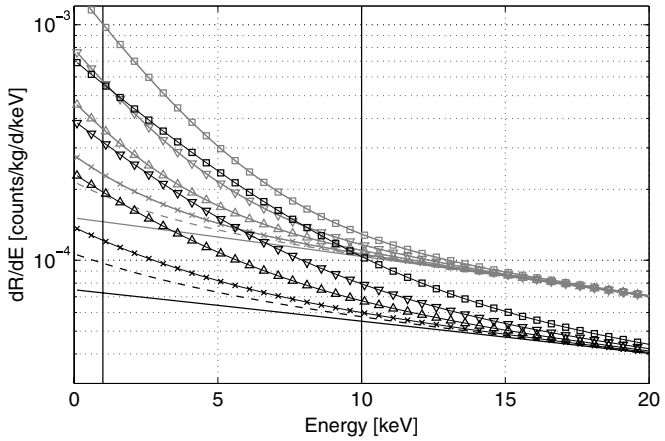

Figure 3. Total differential rate for a Ge target in the SHM (solid) and four different values of ρ_d/ρ_h (0.1 dashed, 0.2 ×, 0.5 △, 1 ▽, and 2 □) are shown for two M_{WIMP} (100 GeV/c^2 (red/gray) and 200 GeV/c^2 (blue/black)). The vertical lines mark the current CDMS-II threshold and a threshold of 1 keV.

The motion of the Earth around the Sun gives rise to an annual modulation of the event rate and recoil energy spectrum (Drukier et al. 1986). The annual modulation is more pronounced for the dark disk, since the relative change to the mean streaming velocity owing to the Earth's motion is larger (∼19%) compared with the SHM (∼6%). We show in Figure 4 the residual integrated rates for a liquid xenon detector throughout a year, for three different M_{WIMP} and two values of ρ_d/ρ_h. The residuals are calculated with respect to the mean counting rates in a given energy region.

The phase (defined at maximum rate) of the dark disk and the SHM differ because the Sun's motion is slightly misaligned to the dark disk. While the phase of each component does not depend on M_{WIMP}, their sum does because their amplitudes depend on M_{WIMP}. We show this dependency in Figure 5, for three values of ρ_d/ρ_h. The phase shift is determined by the relative contributions of each component. Figure 4 shows that the phase shift is largest for low ρ_d/ρ_h, since in this case the sum preferentially follows the halo modulation phase, while for higher ρ_d/ρ_h the disk component dominates the modulation phase. This is a new effect introduced by the presence of the dark disk that allows M_{WIMP} to be uniquely determined from the phase of the modulation signal, for given ρ_d/ρ_h. Note that there is an amplitude flip for the SHM that occurs as M_{WIMP} is increased, which is not seen for the dark disk. As M_{WIMP} is lowered, the "crossing energy" at which the differential rates for minimal and maximal WIMP velocity are equal shifts to lower energies. For the dark disk, it remains close to, or below, current thresholds and so the amplitude flip is not seen.

The effect of the dark disk on current upper limits on the SI WIMP–nucleon cross section is shown in Figure 6 for

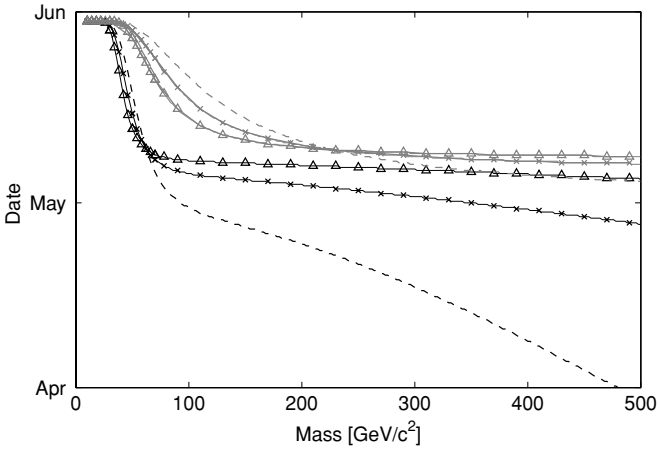

Figure 5. Phase shifts as a function of M_{WIMP} in the energy range reported by the CDMS-II experiment (10–100 keV; red/gray) and the XENON10 experiment (4.5–27 keV; blue/black), for three different values of ρ_d/ρ_h (0.5 dashed, 1 ×, and 2 △).

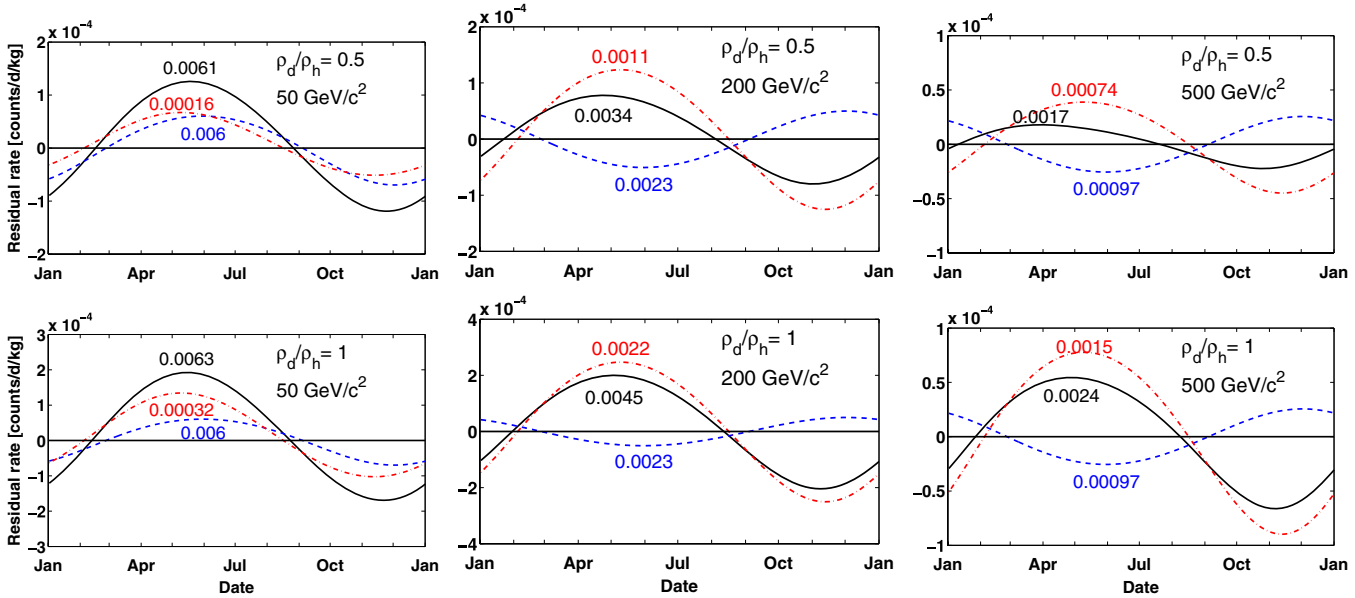

Figure 4. Annual modulation shown as the residual counting rate vs. date for the XENON10 experiment (4.5–27 keV). The residuals are calculated with respect to the mean counting rates (given as numbers over each line) using a WIMP–nucleon cross section of 10^{-8} pb. The top/bottom row is calculated for $\rho_d/\rho_h = 0.5/1$ and M_{WIMP} (left to right) of 50, 200, and 500 GeV/c^2. The (blue/dashed) line is the modulation signal obtained from the SHM, the (red/dot-dashed) line is the modulation signal from the dark disk, and the (black/solid) line is the total modulation signal. The maximum of the dark disk contribution is shifted to May 9th compared with the SHMs maximum/minimum on May 30th. *Note the different vertical scales in each of the three columns of the plot array.*

(A color version of this figure is available in the online journal.)

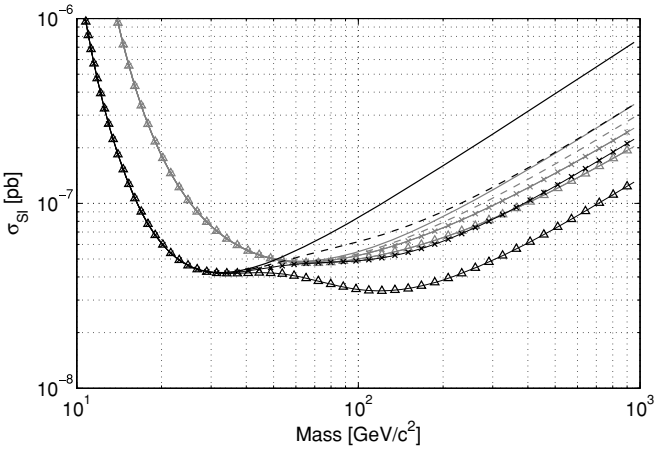

Figure 6. Effect of the increased dark matter flux on the SI WIMP–nucleon cross section constraints obtained by the CDMS-II (red/gray) and XENON10 (blue/black) experiments, for three different values of ρ_d/ρ_h (0.5 dashed, 1 ×, and 2 △). The solid lines give the constraints if only the SHM component is considered.

CDMS-II and XENON10 (Ahmed et al. 2009; Angle et al. 2008). Depending on ρ_d/ρ_h, we exclude new regions in the allowed parameter space for $M_{WIMP} \gtrsim 50$ GeV/c^2.

On a final note, we find that including the dark disk component does not change the interpretation of the annual modulation signal observed in the Dark Matter (DAMA) (Bernabei et al. 2008) experiment for pure SI coupling. At high M_{WIMP}, the allowed DAMA region is still excluded by CDMS-II and XENON10 (Ahmed et al. 2009; Angle et al. 2008) results, while at low M_{WIMP} no new parameter region opens.

3. CONCLUSIONS

In ΛCDM, a dark matter disk forms from the accretion of satellites. We have shown how its low velocity with respect to the Earth alters the expected rate and annual modulation signal in dark matter detectors. Our main findings are as follows.

The dark disk boosts the detection rates at low recoil energy. For $M_{WIMP} \gtrsim 50$ GeV/c^2, recoil energies of 5–20 keV and $\rho_d/\rho_h \leqslant 1$, the rate is boosted by factors up to 2.4 for Ge and 3 for Xe targets. Comparing this with the rates at higher energy will constrain M_{WIMP}, particularly for $M_{WIMP} > 100$ GeV/c^2.

The dark disk has a different annual modulation phase than the dark halo, while the relative amplitude of the two components varies with recoil energy and M_{WIMP}. As a result, there is a new richness in the annual modulation signal that varies uniquely with M_{WIMP}, for given dark disk properties (the properties of the dark disk will be measured from next generation surveys; Steinmetz et al. 2006; Perryman et al. 2001).

The increased expected dark matter flux provides new constraints on the WIMP cross section from current experiments. For likely dark disk properties ($\rho_d/\rho_h \leqslant 1$), the constraints for pure SI coupling improve by up to a factor of 1.4 for CDMS-II (Ahmed et al. 2009) and 3.5 for XENON10 (Angle et al. 2008).

We acknowledge support from the Swiss NSF and the wonderful working environment and support of UZH.

REFERENCES

Aalseth, C., et al. 2008, Phys. Rev. Lett., 101, 251301
Ahmed, Z., et al. 2009, Phys. Rev. Lett., 102, 011301
Angle, J., et al. 2008, Phys. Rev. Lett., 100, 021303
Bahcall, J. 1984, ApJ, 287, 926
Baudis, L. 2006, Int. J. Mod. Phys. A, 21, 1925
Bernabei, R., et al. 2008, Eur. Phys. J. C., 56, 333
Brook, C., Kawata, D., Gibson, B., & Freeman, K. 2004, ApJ, 612, 894
Burstein, D. 1979, ApJ, 234, 829
Cheng, H., Feng, J., & Matchev, K. 2002, Phys. Rev. Lett., 89, 211301
Dehnen, W., & Binney, J. 1999, MNRAS, 298, 387
Drukier, A., Freese, K., & Spergel, D. 1986, Phys. Rev. D, 33, 3495
Ellis, J., et al. 1984, Nucl. Phys. B, 238, 453
Freese, K., Gondolo, P., Newberg, H. J., & Lewis, M. 2004, Phys. Rev. Lett., 92, 111301
Gilmore, G., & Reid, N. 1983, MNRAS, 202, 1025
Goodman, M. W., & Witten, E. 1985, Phys. Rev. D, 31, 3059
Green, A. M. 2002, Phys. Rev. D, 66, 83003
Gunn, J. E., et al. 1978, ApJ, 223, 1015
Holmberg, J., & Flynn, C. 2000, MNRAS, 313, 209
Hooper, D., & Profumo, S. 2007, Phys. Rep., 453, 29
Jungman, G., Kamionkowski, M., & Griest, K. 1996, Phys. Rep., 267, 195
Kamionkowski, M., & Kinkhabwala, A. 1998, Phys. Rev. D, 57, 3256
Kamionkowski, M., & Koushiappas, S. 2008, Phys. Rev. D, 77, 103509
Kazantzidis, S., et al. 2008, ApJ, 688, 254
Lake, G. 1989, AJ, 98, 1554
Lake, G. 1990, Nature, 346, 39
Lee, B., & Weinberg, S. 1977, Phys. Rev. Lett., 39, 165
Lewin, J., & Smith, P. 1996, Astropart. Phys., 6, 87
Lin, S. T., et al. 2009, Phys. Rev. D, 79, 061101
Moore, B., et al. 1998, ApJL, 499, L5
Navarro, J., Frenk, C., & White, S. 1997, ApJ, 490, 493
Oort, J. 1932, Bull. Astron. Soc. Neth., 6, 24
Oort, J. 1960, Bull. Astron. Soc. Neth., 15, 45
Perryman, M., et al. 2001, A&A, 369, 339
Read, J., Lake, G., Agertz, O., & Debattista, V. 2008, MNRAS, 389, 1041
Savage, C., Freese, K., & Gondolo, P. 2006, Phys. Rev. D, 74, 043531
Silk, J., & Srednicki, M. 1984, Phys. Rev. Lett., 53, 624
Smith, M. C., et al. 2007, MNRAS, 379, 755
Statler, T. 1989, ApJ, 344, 217
Steinmetz, M., et al. 2006, AJ, 132, 1645
Yoachim, P., & Dalcanton, J. 2005, ApJ, 624, 701
Yoachim, P., & Dalcanton, J. 2006, AJ, 131, 226